Use of Elastic Full Waveform Inversion for Monitoring of Dams and Levees

Jack Montgomery[1#], *Pourya* Alidoust[2], and *Joseph* Coe[3]

[1]*Auburn University, Department of Civil and Environmental Engineering, Auburn, AL, USA*
[2]*HNTB, 1650 Arch Street, Philadelphia, PA, USA*
[3]*San José State University, Department of Civil and Environmental Engineering, San José, CA, USA*
[#]*Corresponding author: jmontgomery@auburn.edu*

ABSTRACT

Understanding subsurface conditions is critical to creating and maintaining resilient infrastructure systems, such as dams and levees. Seismic geophysical tools can be very effective for site characterization of these structures as they directly measure the elastic moduli and can provide insight into both the soil properties and groundwater conditions. Full waveform inversion (FWI) is one processing option for seismic geophysics that seeks to overcome some of the limitations in the traditional approaches by using the full time-domain recording of the wavefield to develop 2D or 3D profiles of shear wave velocity. In addition to providing characterization data, FWI can also potentially be used as a monitoring tool for dams and levees to assess how elastic moduli are changing with time and to infer how these changes might relate to changes in the hydromechanical properties of the soil. This study seeks to explore the use of seismic FWI as both a characterization and monitoring tool through numerical simulations of seismic surveys on a hypothetical levee with a low velocity anomaly in the foundation. The simulations are used to assess both the spatial resolution and the ability of the simulations to detect changes in properties that might be related to softening of the foundation or development of internal erosion failure modes. The findings from the study will be used to highlight potential benefits and challenges to using seismic FWI for characterization and monitoring of dams and levees.

Keywords: Full waveform inversion, geophysical tests, dams, levees, monitoring

1. Introduction

Dams and levees are critical components of both flood control and water supply infrastructure. These structures are often constructed on alluvial deposits, which can be heterogeneous and susceptible to strength loss and internal erosion. In addition, many older structures were constructed without modern engineering practices, such as filter design and compaction control, leaving them vulnerable to internal erosion with the embankment and/or static liquefaction. Static liquefaction is also a major failure mode for tailings dams, where failures have occurred with little warning.

Site characterization for dams and levees has traditionally relied on borings and in-situ penetration tests (i.e., Standard, Cone, or Becker Penetration Tests) to identify soil layering, collect samples for laboratory tests, and to select strength parameters for analyses. These tools can provide detailed information at the location they are performed, but are inherently one-dimensional (1D) and cannot provide information in unsampled locations. It may also be difficult or expensive to perform repeated sampling to monitor changes over time.

Seismic geophysical tools can be a very effective addition to dam and levee site investigations as they directly measure elastic moduli, which is an engineering property and can provide insight into both the soil properties and groundwater conditions (Dezert et al. 2019). The majority of seismic geophysical methods used in geotechnical applications rely on two forms of analysis: (1) ray-based methods such as seismic reflection/refraction, crosshole methods, and downhole methods; (2) dispersion-based methods such as the spectral analysis of surface waves (SASW) and multichannel analysis of surface waves (MASW). Full waveform inversion (FWI) is an alternative approach that seeks to overcome some of the limitations in the traditional seismic processing approaches by using the full time-domain recording of the wavefield to develop 2D or 3D profiles of shear wave velocity (v_s) (Virieux and Operto 2009). Previous studies have demonstrated the FWI can lead to significant improvements in resolution for near-surface applications (Tran et al. 2013, Kiernan et al. 2021, Coe and Mahvelati 2021, Yust et al. 2023), but more work is needed to undforerstand the resolution of FWI and to explore the ability of FWI to serve as a monitoring tool.

This study seeks to test the ability of seismic FWI to detect small changes in v_s in a layered deposit. Two models are considered that are meant to represent a survey performed near the toe of an embankment (small dam or levee) and a survey performed on the crest of the embankment. The models are meant to represent a permanent or semi-permanent array that is used to track the potential changes in the property of the foundation. Low velocity anomalies are introduced within the foundation layer to represent a softened zone. The magnitude of softening (30%) is selected to represent the

larger end of changes in v_s that might be expected due to internal erosion (Planès et al. 2016, Johnston, Murphy, and Holden 2024) or reductions in effective stress that might signal development of high excess pore pressures (Desai 2000, Zayed et al. 2021).

2. Methods

2.1. Selected Geometry

The problem geometry selected to for this study is shown in Figure 1. This geometry represents a 5-m tall levee on a two-layer foundation. The top layer is considered to be a fine-grained blanket material, while the foundation layer represents a medium-dense sand. This stratigraphy is common underneath levees along the Mississippi River in the United States (Kelley et al. 2020) among other areas. While the selected geometry is three-dimensional (3D), all analyses in this study are 2D.

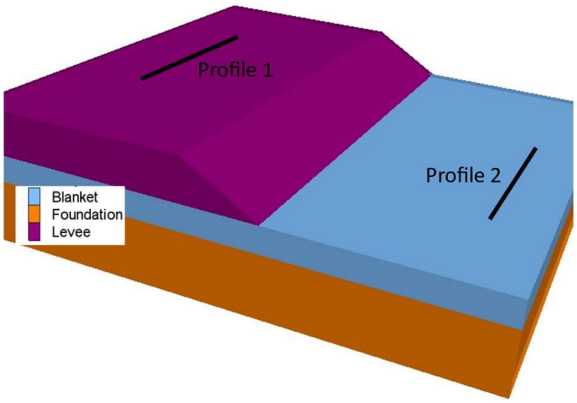

Figure 1. Hypothetical levee used for this study showing the location of the two 2D profiles that are used in the analysis and the layering used in the analysis.

The location of the two 2D profiles are also shown in Figure 1. Profile 1 represents a survey performed on the crest of the levee and includes the 5-m embankment, while profile 2 represents a survey performed at the toe of the levee and does not consider the effect of the embankment. Properties for each of the layers are shown in Table 1. All layers were assumed to be saturated in this study, but the results are not expected to be sensitive to the compression (P) wave velocity (v_p).

Table 1. Properties of the four zones in the true model.

Layer	Thickness (m)	Wave Velocity (m/s)	
		Shear	Compression
Levee	5	300	1,500
Blanket	3	130	1,500
Foundation	7	250	1,500
Softened Zone	1 or 3 m	175	1,500

The cross-sections of the two profiles are shown in Figure 2 and represent the true models for the inversion. A low velocity anomaly is placed at the interface between the blanket and foundation layer to represent the softened zone. The velocity of the softened zone is set at 175 m/s, which represents a 30% reduction in velocity from the initial state of this layer. This difference is consistent with experimental observations from tests on soils undergoing internal erosion (Planès et al. 2016, Johnston, Murphy, and Holden 2024).

The initial models for the inversion process are identical to the true models (Figure 2) with the softened zone removed. This approach assumes that previous studies have been used to fully characterize the existing conditions and the analyses in this study are being used for monitoring or detecting changes from this known initial condition. This level of perfect knowledge of all properties except the softened zone is an ideal case, which serves as a proof of concept for the ability of FWI

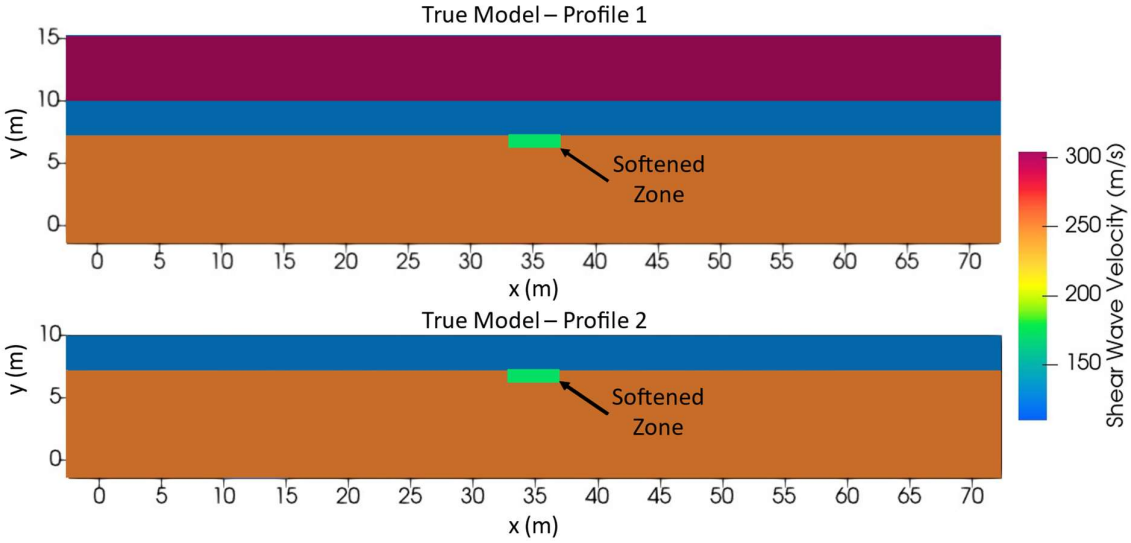

Figure 2. Two-dimensional (2D) profiles used as the true model (1 m x 4 m softened zone) in the forward modelling phase of the FWI process. The model consists of three layers (with the embankment layer omitted from profile 2) and the softened zone (v_s = 175 m/s) at the interface between the foundation (v_s = 250 m/s) and the blanket layer (v_s = 125 m/s).

to detect small, softened zones. Future work will explore effects of heterogeneity and less accurate starting models.

2.2. Forward Modelling

The Salvus***Project*** module of the Salvus software suite (Mondaic®) is utilized in this study for both elastic forward modelling and subsequent inversion of the acquired waveforms (Afanasiev et al. 2019). Salvus uses a spectral-element method (SEM) formulation for solving the equations related to elastic wave propagation. The computational mesh is shown in Figure 3. The elements were approximately 0.7 m tall and used 4th order polynomial shape functions. This size mesh was capable of transmitting frequencies of up to 100 Hz or wavelengths of between 1.3 – 3 m depending on the shear wave velocity. A total of 52 receivers were placed on the surface across each of the profiles in Figure 2. An interval of 1.0 m was used between receivers. This resulted in an array length of 52.0 m that spanned between x = 10.0 m and 61.0 m along the surface of the models. Waveforms were simulated across the profiles by exciting 26 impulse signals as seismic sources on the ground surface. The signals were generated using a vertically polarized Ricker wavelet with a central frequency of 40 Hz. The source signals were spaced 2.0 m apart, starting at x = 10.5 m. Each simulation was performed for 0.4 seconds. This arrangement of sources and receivers closely resembles typical surface wave acquisition schemes used in seismic geophysical testing. Boundary conditions included a free surface at the top of the domain to mimic the ground surface and absorbing boundaries along the sides and bottom (Clayton and Engquist 1977) to remove unwanted and unrealistic reflections caused by the limited size of the domain relative to real world settings.

An example output from receiver 25 (center of array) is shown in Figure 4a for Profile 1 with a 1 m thick and 4 m long softened zone in the foundation layer. The difference between the traces in the time domain is very difficult to see at this scale, but variations occur after 0.15 seconds. To better visualize the difference between the traces, the arithmetic difference between the initial and true model and the final inverted model and the true model, respectively, are shown in Figure 4b.

2.3. FWI Approach

Model parameters were updated during FWI using a quasi-Newton method called the limited-memory Broyden–Fletcher–Goldfarb–Shanno (L-BFGS) algorithm by Nocedal and Wright (2006). This algorithm attempts to approximate the Hessian matrix and balances the gradient to facilitate convergence towards the global minima of the selected objective function [optimal transport misfit (Yang and Engquist 2018)]. Multiple strategies were used in this study to mitigate for the ill-posedness of the inversion problem (i.e., being inherently challenging and mathematically unstable). First, a hierarchical inversion approach was employed that involved the gradual introduction of different frequency components (Bunks et al. 1995). Typically, the inversion process begins with lower frequency sources to establish a lower resolution subsurface profile before higher frequencies are introduced to identify smaller features present in the subsurface profile. Specifically, in this study the inversion process commenced with a Ricker wavelet source with central frequency of 20 Hz, followed by 30 Hz, 40 Hz, and eventually 50 Hz. Each of these stages of the inversion process continued until there was no further improvement in the misfit value for all the source events. It was also assumed that the intact embankment and foundation layers were well characterized so that the initial model used during inversion already accurately predicted the wave velocities of these strata. In addition to these a-priori assumptions, regularization was applied during inversion as a smoothing operator on the model parameters (Gaussian smoothing with halfwidth of 0.35 m in horizontal direction and 0.25 m in vertical direction). This effort stabilized the inversion from the effects of small-scale heterogeneous features that can generate overly complex wavefields and lead to inversion failure when attempting to fit these wavefields (Boehm et al. 2016).

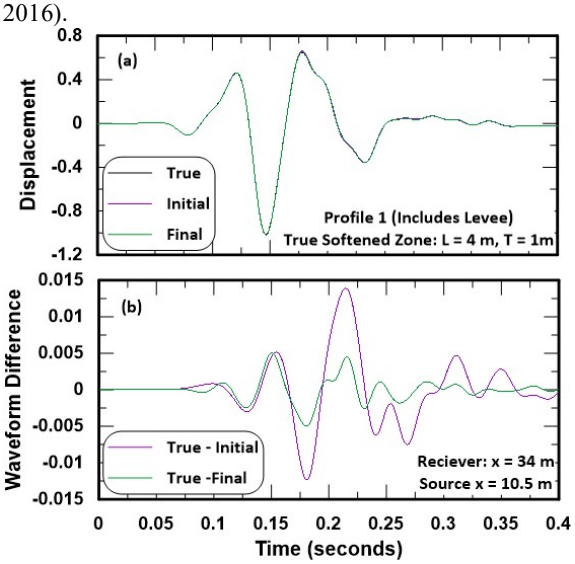

Figure 4. Output from receiver 25 (x = 34 m) showing (a) the recorded traces from the true, initial, and final inverted models and (b) the arithmetic difference between both the initial and final models and the true model. Results are shown for the first source (x = 10.5 m).

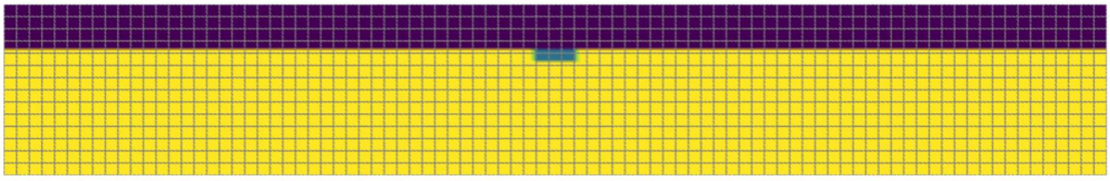

Figure 3. Computational mesh for the FWI simulations using profile 2 and the true model (1 m x 4 m softened zone).

The forward and inverse modelling were executed remotely in parallel modes by using the High-Performance Computing (HPC) resources at Temple University to manage the associated high computational costs. These computations were submitted to ten cores of the compute servers of the Temple HPC cluster for each modelling. Compute is an interactive-use server that provides 88 CPU cores [Intel® Xeon Gold 6238 (Cascade Lake) processors] with up to 1.5 TB of RAM and 0.5 PB shared memory.

3. Results

The outputs from the Salvus***Project*** module include traces from individual receivers (Figure 4b), grid files with gradients from the FWI, and inverted models of v_s, v_p, and density. For this study, only inverted v_s profiles are presented for the sake of brevity.

3.1. Inversion Results

The inverted v_s model for Profile 1 is shown in Figure 5 for a 4 m long ($L_{softened,True}$) softened zone with thicknesses ($T_{Softened,True}$) of either 1 m or 3 m. For both models, the area of the softened zone is clearly observed at the correct location, although with different dimensions (discussed further in the next section). The minimum velocity for the model with $T_{Softened,True}$ = 1 m has a minimum v_s of 187 m/s within the inverted softened zone, while the model with the thicker softened zone ($T_{Softened,True}$ = 3 m) has a minimum v_s of 179 m/s within the inverted softened zone. This is compared with the true v_s of 175 m/s in the softened zone. The minimum v_s value from the inversion is likely to be a function of the smoothing parameters and future work will look at the effect of the smoothing parameters on both the spatial resolution and the magnitude of the softened velocity.

The inverted v_s model for profile 2 is shown in Figure 6 for the same softened zone parameters ($L_{softened,True}$ = 4 m and $T_{Softened,True}$ = either 1 m or 3 m) as profile 1. For

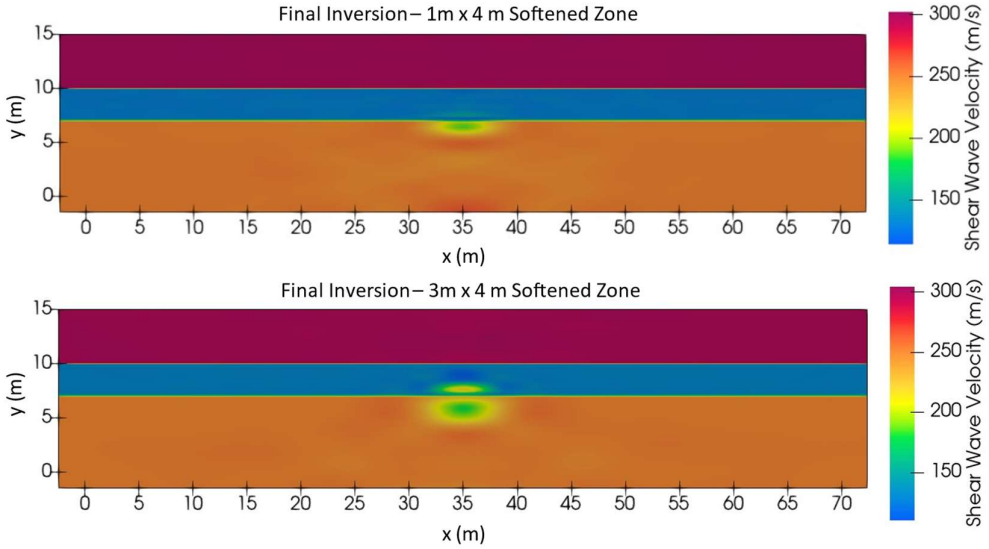

Figure 5. Final v_s inversion results for profile 1 showing the detection of the softened zone within the foundation layer. The other layers are correctly left unchanged in the inversion with the exception of a small zone with increased velocity can also be observed in the blanket layer above the softened zone.

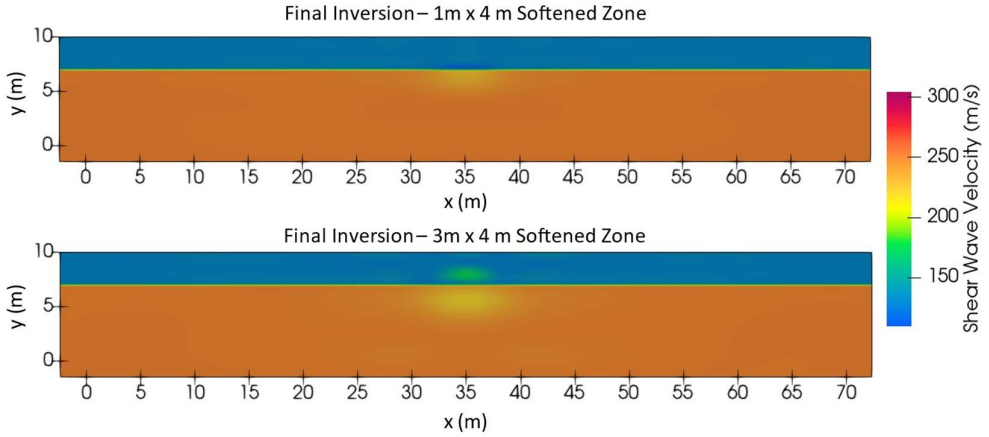

Figure 6. Final v_s inversion results for profile 2 showing the detection of the softened zone within the foundation layer. The other layers are correctly left unchanged in the inversion with the exception of a small zone with increased velocity can also be observed in the blanket layer above the softened zone.

profile 2, the softened zone is much harder to observe, although a reduction in velocity is observed at the correct location in both models. The model with $T_{Softened,True}$ = 1 m has a minimum v_s of 225 m/s within the inverted softened zone, while the model with the thicker softened zone ($T_{Softened,True}$ = 3 m) has a minimum v_s of 217 m/s within the inverted softened zone. Both of these are much larger than the true v_s of 175 m/s. The relatively poor resolution of the softened zone in profile 2 compared with profile 1 may be due to the frequency of the source function. Adding higher frequency sources may help improve these results for shallow features and this will be explored in future work.

Another interesting inversion result is the presence of a zone of increased velocity within the blanket layer directly above the softened zone. This zone is present in all four inverted models, but is most pronounced in the models with the thicker softened zone. This higher velocity region was not in the true model. Previous studies have also found that higher velocity regions can be observed above voids (low velocity anomalies) in seismic surveys. Mirzanejad et al. (2021) used 3D FWI to examine voids in karstic limestone and found that a high velocity zone was located above the void in their inversion. They attributed this increase in velocity to a change in materials at this depth. The results in this study suggest that this zone of higher velocity may also be due to the inversion process. Additional work is needed to determine which factors influence the presence of this zone of increased v_s.

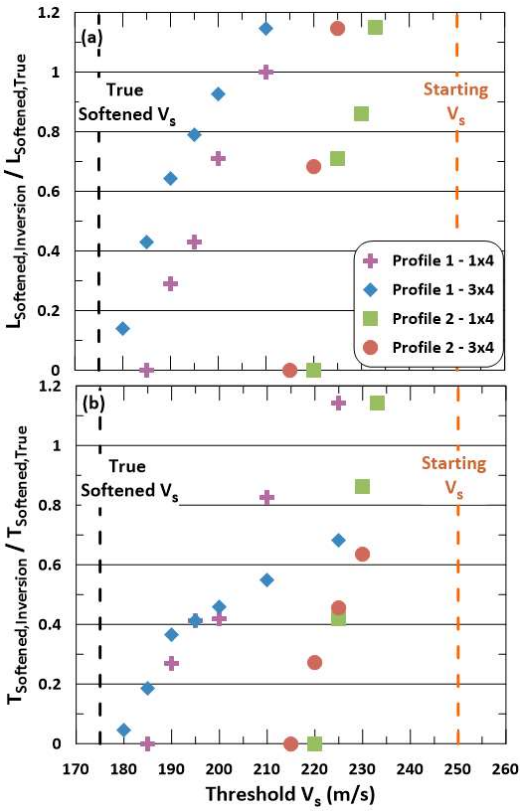

Figure 7. Normalized (a) length and (b) thickness of the softened zone from the inverted v_s model. The dimensions of the softened zone from the inverted model are computed for different velocity thresholds to separate unchanged zones from softened zones in the foundation and the dimensions are normalized by the true dimensions (i.e., a normalized value of 1.0 the same as the true model).

3.2. Size of Softened Zone from FWI Results

The inverted v_s results were post-processed using ParaView to extract the size of the softened zone from FWI. These results are shown in Figure 7 for both profiles (with and without the embankment) and both thicknesses of the true softened zone (1 m or 3 m). The results are presented in terms of the length of the softened zone in the inverted model ($L_{Softened,Inversion}$) normalized by the true length ($L_{Softened,True}$) in Figure 7a and the thickness of the softened zone in the inverted model ($T_{Softened,Inversion}$) normalized by the true thickness ($T_{Softened,True}$) in Figure 7b. The dimensions of the softened zone in the inverted model were measured by calculating the maximum horizontal and vertical distances (for length and thickness, respectively) between elements with a velocity that was lower than the selected threshold value for softening. The true v_s of the softened zone is 175 m/s, but none of the inverted models contained zones with this velocity within the foundation layer. Therefore, the threshold velocity needed to be greater than 175 m/s, but lower than the starting v_s of 250 m/s. Various threshold values were considered between these limits.

Using a velocity threshold of 200 m/s would provide a good estimate of the true length of the softened zone for profile 1 (Figure 7a), while a threshold value of 225 m/s would be needed to get a similar level of agreement for profile 2. Using the higher threshold for profile 1 would lead to an overestimate of the length. Using thresholds of 200 m/s for profile 1 and 225 m/s for profile 2 would lead to an inverted thickness that is approximately 40-50% of the true value for all four cases (Figure 7b). These results demonstrate that there is no simple way to select a threshold velocity for measuring the dimensions of the softened zone from these FWI results.

4. Discussion

The dimensions of the softened zone in the inverted models were extracted using different velocity thresholds to distinguish which zones have changed. Using a threshold v_s of 200 m/s (a reduction of 20% from the starting v_s compared with the true reduction of 30%) provided a reasonable estimate of the true length of the softened zone in profile 1 but would underestimate the thickness by approximately 50%. None of the zones in the inversion for profile 2 had a v_s less than 215 m/s and therefore the softened zone would not be detected using this threshold. A threshold v_s of 225 m/s (reduction of 10% from the starting v_s) would need to be applied to profile 2 to get a similar level of detection.

The results show that the FWI approach used in this study, which used a similar procedure to traditional surface wave surveys, can detect the softened zone for surveys on the crest of the levee (profile 1). This approach is unlikely to be able to distinguish the softened zone from other sources of variability for surveys at the toe of a levee (profile 2). To improve the resolution for shallow depths (~3 m), the survey design may need to be

adjusted to use higher frequency sources and closer receiver spacing. Additional work is needed to explore how changes in survey and inversion parameters affect the spatial resolution of FWI for dams and levees.

This study has only considered 2D elastic FWI and does not include attenuation or 3D effects. The starting model for the FWI was also in perfect agreement with the true model, except for the presence of the softened zone. Having a perfect starting model will not be possible in real surveys. Similarly, real soil layers will not have uniform properties as are considered in this study. Therefore, the current results should be considered a proof of concept for the potential of seismic FWI to detect relatively small zones of softening, such as those that may be caused by internal erosion or significant decreases in effective stress. Future work is needed to see how this detection ability changes with the introduction of realistic variability in properties and stratigraphy. The authors plan to explore this in future studies.

5. Conclusions

There are currently no accepted approaches to continuously monitor the development of internal erosion or high excess pore pressures that may lead to static liquefaction within or beneath dams and levees. Both failure modes lead to reductions in shear stiffness (and therefore shear wave velocity), but the magnitude of the reduction and the size of the affected area is often too small to be detected with traditional monitoring approaches. The authors believe the seismic FWI using permanent or semi-permanent arrays of seismic sources and receivers has the potential to be used for this purpose.

This study presented results from seismic FWI analyses applied to a hypothetical levee with a softened zone in the foundation. The starting model for the inversion used uniform layering and properties, while the true model included a zone with a 30% reduction in v_s. The inverted v_s models for surveys performed on the crest of the levee were able to detect the presence of the softened zone at a depth of 8 m with good agreement in terms of the length, although the thickness of the zone was smaller. The inverted v_s models for surveys performed at the toe of the levee also showed the presence of the softened zone at a depth of 3 m, but the dimensions of the softened zone and the magnitude of the v_s reduction were much smaller than the true model.

The results demonstrate that seismic FWI can detect v_s reductions of approximately 30% below a hypothetical levee. The survey parameters used in this analysis are similar to those used in traditional surface wave surveys and the FWI resolution could likely be improved through optimization of these parameters, including source characteristics and receiver spacing. Additional work is also needed to determine how including 3D effects, attenuation, heterogeneity, and alternative starting models affect the results. The authors plan to explore these effects in future studies.

Acknowledgements

The first author received support from the National Science Foundation under grant number CMMI 2047402. This research also includes calculations conducted on Temple University's HPC resources and thus was supported in part by the National Science Foundation through major research instrumentation grant number 1625061 and by the US Army Research Laboratory under contract number W911NF-16-2-0189. Any opinions, findings, conclusions, or recommendations are those of the author(s) and do not necessarily reflect the views of the National Science Foundation and US Army Research Laboratory.

References

Afanasiev, M., C. Boehm, M. van Driel, L. Krischer, M. Rietmann, D. A. May, M. G. Knepley, and A. Fichtner. 2019. "Modular and Flexible Spectral-Element Waveform Modelling in Two and Three Dimensions." *Geophysical Journal International* 216 (3): 1675–92. https://doi.org/10.1093/gji/ggy469.

Boehm, C., M. Hanzich, J. De La Puente, and A. Fichtner. 2016. "Wavefield Compression for Adjoint Methods in Full-Waveform Inversion." *GEOPHYSICS* 81 (6): R385–97. https://doi.org/10.1190/geo2015-0653.1.

Bunks, C., F. M. Saleck, S. Zaleski, and G. Chavent. 1995. "Multiscale Seismic Waveform Inversion." *GEOPHYSICS* 60 (5): 1457–73. https://doi.org/10.1190/1.1443880.

Clayton, R., and B. Engquist. 1977. "Absorbing Boundary Conditions for Acoustic and Elastic Wave Equations." *Bulletin of the Seismological Society of America* 67 (6): 1529–40. https://doi.org/10.1785/BSSA0670061529.

Coe, J. T., and S. Mahvelati. 2021. "Full Waveform Tomography to Address Challenges with Surface Wave Dispersion Information Caused by Significant Stochastic Variability of Subsurface Stiffness." *Journal of Environmental and Engineering Geophysics* 26 (4): 267–78. https://doi.org/10.32389/JEEG21-013.

Desai, C. S. 2000. "Evaluation of Liquefaction Using Disturbed State and Energy Approaches." *Journal of Geotechnical and Geoenvironmental Engineering* 126 (7): 618–31. https://doi.org/10.1061/(ASCE)1090-0241(2000)126:7(618).

Dezert, T., Y. Fargier, S. Palma Lopes, and P. Côte. 2019. "Geophysical and Geotechnical Methods for Fluvial Levee Investigation: A Review." *Engineering Geology* 260 (October): 105206. https://doi.org/10.1016/j.enggeo.2019.105206.

Johnston, I., W. Murphy, and J. Holden. 2024. "The Effects of Internal Erosion on Granular Soils Used in Transport Embankments." *Soils and Foundations* 64 (1): 101424. https://doi.org/10.1016/j.sandf.2024.101424.

Kelley, J. R., K. B. Parkman, J. B. Dunbar, R. C. Strange, B. R. Breland, I. J. Stephens, E. R. Gore, and M. K. Corcoran. 2020. "Study of Sand Boil Development at Kaskaskia Island, IL, Middle Mississippi River Valley." ERDC TR-20-19. Geotechnical and Structures Laboratory, U.S. Army Engineer Research and Development Center.

Kiernan, M., D. Jackson, J. Montgomery, J. B. Anderson, B. W. McDonald, and K. C. Davis. 2021. "Characterization of a Karst Site Using Electrical Resistivity Tomography and Seismic Full Waveform Inversion." *Journal of Environmental and Engineering Geophysics* 26 (1): 1–11. https://doi.org/10.32389/JEEG20-045.

Mirzanejad, M., K. T. Tran, M. McVay, D. Horhota, and S. J. Wasman. 2021. “Deep Void Detection with 3D Full Waveform Inversion of Surface-Based and in-Depth Source Seismic Wavefields.” *Engineering Geology* 294 (December): 106407. https://doi.org/10.1016/j.enggeo.2021.106407.

Nocedal, J., and S. J. Wright. 2006. *Numerical Optimization*. Second edition. Springer Series in Operation Research and Financial Engineering. New York, NY: Springer.

Planès, T., M. A. Mooney, J. B. R. Rittgers, M. L. Parekh, M. Behm, and R. Snieder. 2016. “Time-Lapse Monitoring of Internal Erosion in Earthen Dams and Levees Using Ambient Seismic Noise.” *Géotechnique* 66 (4): 301–12. https://doi.org/10.1680/jgeot.14.P.268.

Tran, K. T, M. McVay, M. Faraone, D. Horhota. 2013. “Full Seismic Waveform Tomography at a Highly Variable Florida Site.” In , Transportation Research Board 92nd Annual Meeting Washington DC, USA, 14p.

Virieux, J., and S. Operto. 2009. “An Overview of Full-Waveform Inversion in Exploration Geophysics.” *GEOPHYSICS* 74 (6): WCC1–26. https://doi.org/10.1190/1.3238367.

Yang, Y., and B. Engquist. 2018. “Analysis of Optimal Transport and Related Misfit Functions in Full-Waveform Inversion.” *GEOPHYSICS* 83 (1): A7–12. https://doi.org/10.1190/geo2017-0264.1.

Yust, M. B. S., B. R. Cox, J. P. Vantassel, P. G. Hubbard, C. Boehm, and L. Krischer. 2023. “Near-Surface 2D Imaging via FWI of DAS Data: An Examination on the Impacts of FWI Starting Model.” *Geosciences* 13 (3): 63. https://doi.org/10.3390/geosciences13030063.

Zayed, M., A. Ebeido, A. Prabhakaran, K. Kim, Z. Qiu, and A. Elgamal. 2021. “Shake Table Testing: A High-Resolution Vertical Accelerometer Array for Tracking Shear Wave Velocity.” *Geotechnical Testing Journal* 44 (4): 1097–1118. https://doi.org/10.1520/GTJ20190066.